



**HAL**  
open science

## Investigation of LiNbO<sub>3</sub> and LiTaO<sub>3</sub> single crystals for pyroelectric applications in the wide temperature range

Svetlana L Bravina, Nicholas V Morozovsky, Anna N Morozovska, Stéphane Gille, Jean-Paul Salvestrini, Marc Fontana

► **To cite this version:**

Svetlana L Bravina, Nicholas V Morozovsky, Anna N Morozovska, Stéphane Gille, Jean-Paul Salvestrini, et al.. Investigation of LiNbO<sub>3</sub> and LiTaO<sub>3</sub> single crystals for pyroelectric applications in the wide temperature range. *Ferroelectrics*, 2007, 353, pp.636-645. 10.1080/00150190701368166 . hal-00186014

**HAL Id: hal-00186014**

**<https://hal.science/hal-00186014>**

Submitted on 2 Dec 2021

**HAL** is a multi-disciplinary open access archive for the deposit and dissemination of scientific research documents, whether they are published or not. The documents may come from teaching and research institutions in France or abroad, or from public or private research centers.

L'archive ouverte pluridisciplinaire **HAL**, est destinée au dépôt et à la diffusion de documents scientifiques de niveau recherche, publiés ou non, émanant des établissements d'enseignement et de recherche français ou étrangers, des laboratoires publics ou privés.



Distributed under a Creative Commons Attribution - NonCommercial 4.0 International License

# Investigations of $\text{LiNbO}_3$ and $\text{LiTaO}_3$ Single Crystals for Pyroelectric Applications in the Wide Temperature Range

S. L. BRAVINA,<sup>1</sup> N. V. MOROZOVSKY,<sup>1</sup>  
A. N. MOROZOVSKA,<sup>1</sup> S. GILLE,<sup>2</sup> J.-P. SALVESTRINI<sup>2,\*</sup>  
AND M. D. FONTANA<sup>2</sup>

<sup>1</sup>Institute of Physics NASU, 46, Prospect Nauki, 03028 Kyiv, Ukraine,

<sup>2</sup>Laboratoire Matériaux Optiques, Photonique et Systèmes, CNRS UMR 7132, University of Metz and Supélec, 2 rue E. Belin, 57070 Metz, France

*We present temperature dependences of pyroelectric response in  $\text{LiNbO}_3$  and  $\text{LiTaO}_3$  single crystals in operating condition as pyroelectric detectors and in the range 4,2–400 K. In the range 200–400 K, the pyroelectric response is nearly constant. At low-temperature (40–80 K) the pyroelectric response is shown to be the largest. In the range 4,5–12 K, the sign of the pyroelectric coefficient is found to change. This could be used for temperature stabilization devices.*

**Keywords** Low temperatures; lithium niobate; lithium tantalate; pyroelectric phenomena; pyroelectric detectors

## 1. Introduction

Lithium niobate,  $\text{LiNbO}_3$  (LN) and lithium tantalate,  $\text{LiTaO}_3$  (LT) crystals are widely used ferroelectric materials due to their unique electro-optical, non-linear, piezoelectric and pyroelectric properties [1–3].

The development of high sensitive reliable sensors operating in severe conditions has become one of the most important tasks of all branches of modern sensors including pyroelectric sensing at low temperatures [2, 4, 5–8]. For example, security or space IR monitoring where LT and LN crystals are recognized as basic materials for sensitive elements (SE) of pyroelectric detectors of radiation (PDR), requires larger temperature range operation in the mode of thermal cycling and/or thermal impacts.

In this paper, we report in detail and in the frame of various pyroelectric applications, the study of several peculiarities in the temperature behavior (in the range 4,2–400 K) of the pyroelectric response and dielectric permittivity in LN and LT single crystals.

## 2. Experimental

### 2.1. Samples

Single domain Z-cut plates of LN and LT with a thickness of 100-200  $\mu\text{m}$  and an area of 20–50  $\text{mm}^2$  were cut out and polished from a commercial single crystal. The main faces were electroded with evaporated gold and current-carrying wires of a thickness about 0,05 mm were connected to the electrodes with silver-paste. For photopyroelectric measurements the electrodes were covered with thin layer of dispersed gold (Au-black) on which the modulated IR flux was focused.

### 2.2. Measurements

Recording of pyroelectric response was performed by photothermomodulation method [6, 7]. The samples under investigation were illuminated by a sine modulated IR light-beam (0,9–5  $\mu\text{m}$ ) with an intensity varying in the range 1  $\mu\text{W}/\text{mm}^2$ –1  $\text{mW}/\text{mm}^2$ . The induced pyroelectric response amplitude  $U_\pi$  and phase  $\varphi_\pi$  were measured as function of the temperature in the two modes of PDR operation, namely pyroelectric current mode when  $U_\pi = U_{\pi 1} \propto \gamma/c_1$  and pyroelectric voltage mode when  $U_\pi = U_{\pi 2} \propto \gamma/c_1 \varepsilon f_m$ .  $\gamma$  is the pyroelectric coefficient,  $c_1$  is the volume heat capacity,  $\varepsilon$  is the dielectric permittivity, and  $f_m$  is the frequency of the thermal flux modulation. Such operation under the condition  $\varphi_{\pi 2} - \varphi_{\pi 1} = 90^\circ$  allows the estimation of the value of  $\varepsilon_\pi$  from pyroelectric measurements [7, 8] by using the relation  $D_\pi = U_{\pi 1}/U_{\pi 2} f_m \propto \varepsilon_\pi$  where  $D_\pi$  is the dielectric ratio. The measurement technique and the setup used for the measurements of  $U_\pi$  and  $\varphi_\pi$  are presented in references [6, 7].

For the characterizations in the range 4,2-300 K, the samples were placed in an optical N–He gas-flow cryostat. In the range 300–400 K the samples were placed in an electrically screened cell. The measurements were performed under a temperature variation rate of 0,1 K/min at low temperature and of 1 K/min at room temperature.

The pyroelectric coefficient was determined separately in the range 290–340 K by using the Byer–Roundy method [9] in which the pyroelectric coefficient is given by  $\gamma = (dQ/dt)/A(dT/dt)$ .

The temperatures of both the Peltier element and sample surface were controlled and measured with an accuracy of about  $\pm 0,1$  K using a calibrated copper-constantan thermocouple. A Keithley 617 electrometer was used to measure the pyroelectric charges. The samples were firstly short-circuited to minimize the surface charges.

## 3. Results

### 3.1. Low Temperature Behavior

The temperature dependences of  $U_{\pi 1,2}(T)$ ,  $\varphi_{\pi 1,2}(T)$  and  $D_\pi(T)$  in LN and LT crystals are presented in Figs. 1a and 1b. Although the appearance temperature of the phenomena is not the same for each crystal, we can notice for both crystals the following observations:

- double 180°-change of  $\varphi_{\pi 1,2}(f_m)$  followed by peculiarities of  $\varepsilon_\pi(T)$  near  $T_{01} = 5,5$  K and  $T_{02} = 11$  K for LN and near  $T_{01} = 6,5$  K and  $T_{02} = 9$  K for LT;
- change of  $U_{\pi 1,2}(T)$  dependence near  $T_s \approx 20$ –25 K for LN and LT accompanied by  $\varepsilon_\pi(T)$  peculiarity;

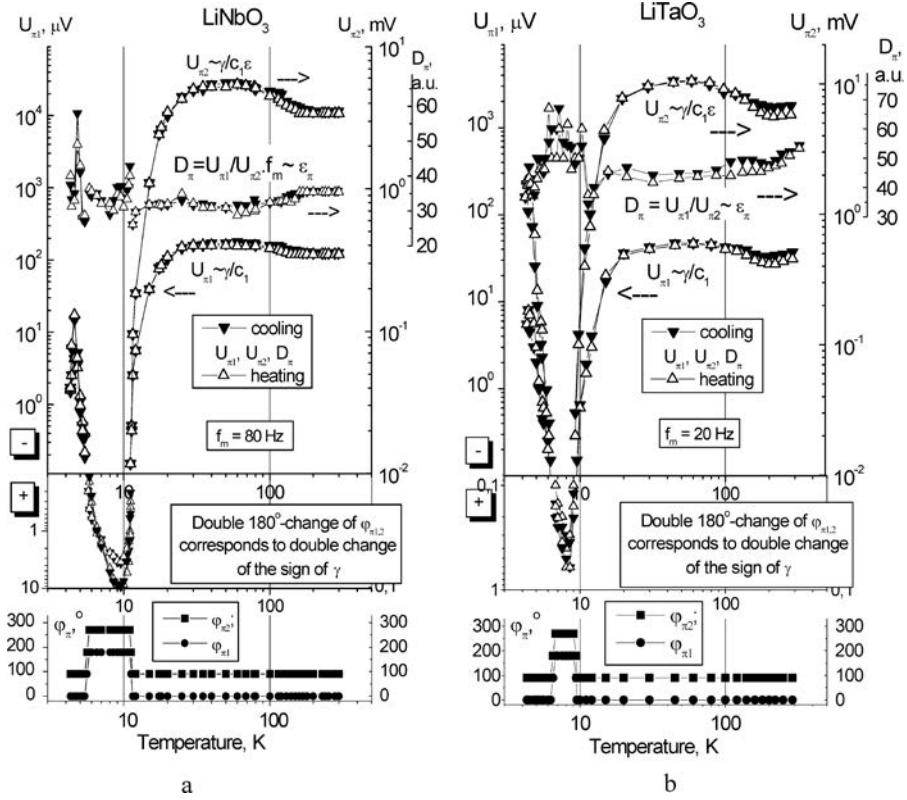


**Figure 1.** Temperature dependences of  $U_{\pi 1,2}$ ,  $D_{\pi}$  and  $\varphi_{\pi 1,2}$  for LiNbO<sub>3</sub> (a) and LiTaO<sub>3</sub> (b) under cooling and heating runs in the temperature range of 4,2–295 K.

- existence of three maxima of the absolute value of  $U_{\pi 1,2}$ , namely small sharp maximum below  $T_{01}$ , small diffuse one between  $T_{01}$  and  $T_{02}$  and large diffuse maximum at  $T_m \approx 50\text{--}60$  K for LN and LT crystals;
- diffuse minimum of  $U_{\pi 1,2}(T)$  and smooth break  $\varepsilon_{\pi}(T)$  dependences in the large vicinity of  $T^* \approx 200$  K for both LN and LT;
- difference in  $U_{\pi 1,2}(T)$  and  $\varepsilon_{\pi}(T)$  variation under cooling and subsequent heating which increases with increasing temperature above  $T_s$ .

The obtained results are in a good agreement with known literature data concerning the peculiarities of pyroelectric [2, 4], piezoelectric [10] and thermophysical [1] characteristics near (5–10) K, 25 K and 200 K discussed in detail in [8]. The correlation in the temperature behavior of electrophysical and thermophysical (in particular thermal expansion and conductivity [1]) characteristics recorded independently indicates the general character of these peculiarities for different LN and LT crystals.

During the cooling and heating cycle at a rate larger than 3 K/min the jump-like behavior of  $U_{\pi 2}$  was found to decrease and to be accompanied by  $\varphi_{\pi 2}$  break. Between jumps of  $U_{\pi 2}$  its smooth increase in time was registered. This amplitude variation of the jump is observed in the case of large temperature change rate and is maximal in the vicinity of 200 K.

The frequency dependences of  $U_{\pi 1}(f_m)$ ,  $U_{\pi 2}(f_m)$ ,  $U_{\pi 2}(f_m) \cdot f_m$  and  $D_{\pi}(f_m)$  (Fig. 2) indicate that the pyroactivity exhibits an uniform distribution. High-frequency decrease of

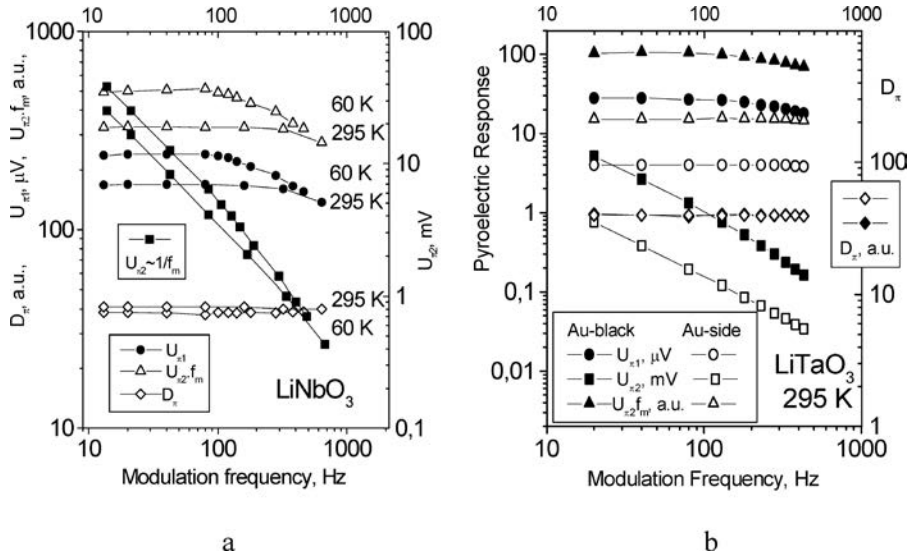


**Figure 2.** Modulation frequency dependences of  $U_{\pi 1}$ ,  $U_{\pi 2}$ ,  $U_{\pi 2} \cdot f_m$  and  $D_{\pi}$ : (a) for LiNbO<sub>3</sub> at different temperatures; (b) for LiTaO<sub>3</sub> under excitation of Au-black and Au-electrode sides.

$U_{\pi 1}(f_m)$  and  $U_{\pi 2}(f_m)$  especially at low temperatures (Fig. 2a), could be connected with the finite value of thermal conductance of Au-black layer (Fig. 2b).

After the thermal cycle 295-4.2-295 K the final values of  $U_{\pi 1,2}$  are weaker than the initial ones. In contrary, the  $\varepsilon_{\pi}$  value is higher than the initial one. During annealing at elevated temperatures transient needle-like pulses of current were observed.

### 3.2. Moderate Temperature Behavior

Figures 3a and 3b show the dependences  $U_{\pi 1,2}(T)$  and  $D_{\pi}(T)$  obtained for LN and LT samples under heating-cooling run in the range of 10-110 °C. In Fig. 4 the temperature dependences of pyroelectric charge release and of pyroelectric coefficient in LN in the range 20–60 °C are presented. The observed changes in  $U_{\pi 1,2}(T)$  and  $D_{\pi}(T)$  correspond to relatively slight changes of  $\gamma/c_1$ ,  $\gamma/c_1\varepsilon$  and  $\varepsilon_{\pi}$  for LN and for LT. The data are in a good agreement with the results obtained in the quasi-static pyroelectric measurements in LN. The same slope of temperature dependences of pyroelectric charges release (Fig. 4, left) corresponds to a slight change of pyroelectric coefficient (Fig. 4 right). Jump-like changes in the temperature dependences of charges release (Fig. 4 left) correspond to peaks of the pyroelectric coefficient (Fig. 4 right). These phenomena observed even under low value of  $dT/dt = 1$  K/min correspond to the appearance of the thermally stimulated non-stationary currents (TSNC) pulses (see 4.1).

The pyroelectric characterization of LN crystals with various doping ions in the temperature range 283–323 K demonstrate that the pyroelectric coefficient values are weakly dependent on LN doping and are close to  $-7 \cdot 10^{-5}$  C/m<sup>2</sup>K. The results are presented in Table 1.

The weak influence of doping on the pyroelectric coefficient value of LN evidences the predominant role of intrinsic defects formed during crystal growth.

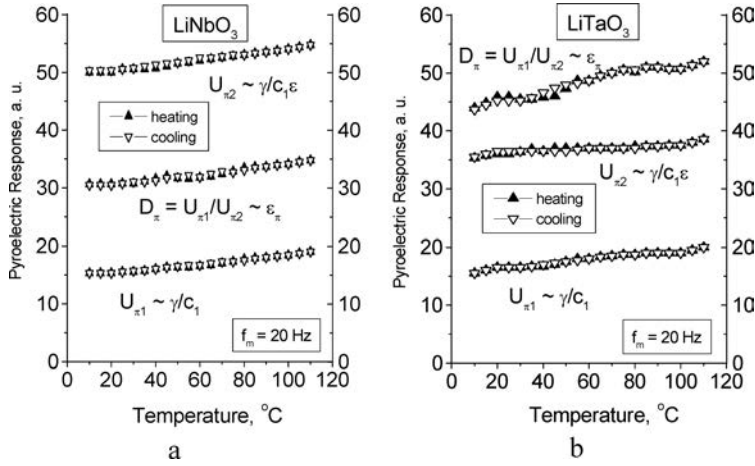


**Figure 3.** Temperature dependences of  $U_{\pi 1,2}$  and  $D_{\pi}$  for LiNbO<sub>3</sub> (a) and LiTaO<sub>3</sub> (b) under heating and cooling runs in the range of 10-110°C.

## 4. Some Application Possibilities

### 4.1. Stability of Pyroelectric Parameters

The expansion of the temperature range for PDR operation requires the examination of the problem of the stability and of the restoration of the PDR characteristics after thermal cycling.

Under cooling and heating runs, for LT as well as for LN [8], TGS [11] and Li<sub>2</sub>GeO<sub>3</sub> [12], thermally stimulated light emission (TSLE) and TSNC phenomena were observed. The change of the shape of low-temperature peculiarities of TSLE- and TSNC- thermograms under cooling and subsequent heating (so under the change of  $dT/dt$  sign) indicates a link with the pyroelectric effect.

For the investigated samples of LN and LT after finishing the 293-4,2-293 K cycle, an apparent decrease of  $U_{\pi 1,2}$  and  $D_{\pi}$  takes place (Fig. 1). However this decrease for LN and LT is less significant than in the case of single crystal samples of TGS [11], Li<sub>2</sub>GeO<sub>3</sub> [12] and Sn<sub>2</sub>P<sub>2</sub>S<sub>6</sub> [13] investigated earlier. Increasing the temperature change rate from 1 to

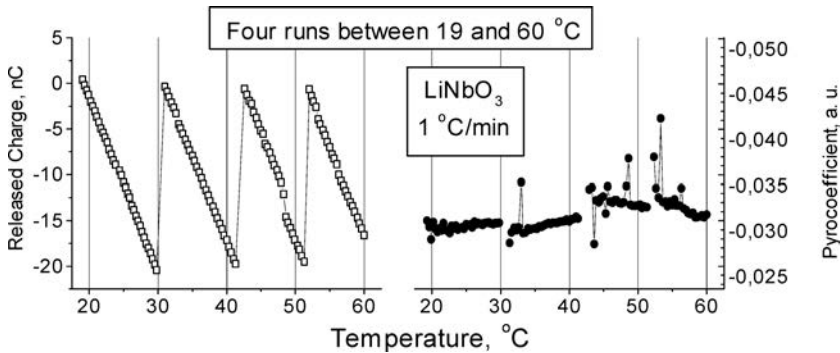


**Figure 4.** Temperature dependences of pyroelectric charge release (left) and pyroelectric coefficient (right) for LiNbO<sub>3</sub> in the range 20-60°C

**Table 1**Pyroelectric coefficient  $\gamma$  [C/m<sup>2</sup> K] of LN crystals with various additives

Pure congruent	$-7 \pm 0, 5$
Stoichiometric	$-6, 7 \pm 0, 5$
0,03% Fe ( $\text{Fe}^{3+}/\text{Fe}^{2+} = 0.2$ )	$-7, 7 \pm 0, 5$
2,2% Zn	$-6, 8 \pm 0, 5$
6% LN ZN	$-7 \pm 0, 5$
8,5% Zn	$-6, 9 \pm 0, 5$
9,6% Zn	$-7, 1 \pm 0, 5$
Mg, Cr [Mg] = $7 \cdot 10^{-2}$ mole/mole ( $\text{Mg}^{2+}/\text{Nb}^{4+}$ ) [Cr] = $3 \cdot 10^{-4}$ mole/mole ( $\text{Cr}^{3+}/\text{Nb}^{5+}$ )	$-7, 8 \pm 0, 5$
5% MG	$-6, 6 \pm 0, 5$

5 K/min results in increasing the difference between initial and final values of  $U_{\pi 1,2}$  and  $D_{\pi}$ . The restoration of the initial state after deep cooling (cryogenic treatment) for all the materials is accompanied by a characteristic pulse noises [11, 13] which are needle-like for LN.

TSLE [14] and TSLE together with TSNC [8] as thermally stimulated electronic emission [15] and other non-stationary phenomena [8, 11-13] are the consequence of the generation of high value of pyroelectric field  $E_{\pi} \sim 10^6$  V/m by pyroactive LN and LT crystals under temperature change ( $E_{\pi} = (\gamma/\epsilon\epsilon_0)(dT/dt) \cdot t_0$ ,  $t_0$  is the duration of the temperature change). The effect of such electric fields leads to external (near the surface) and to internal (in the volume) breakdown and also to polarization reversal which results in more or less pronounced fatigue and degradation of pyroelectric properties [6, 8, 11–13]. This results, in the formation of both free charge carriers and pyroelectrically damaged micro-regions with modified structure. The lower the value of  $dT/dt$  is, the higher the value of  $t_0$  is required to reach the coercive or breakdown values for  $E_{\pi}$ . The existence of a non-zero leakage currents assists the relaxation of accumulated charges and so minimizes the quantity of the pyro-breakdown events for the unit temperature interval.

#### 4.2. Wide Moderately Low-Moderately High Temperature Range PDR

The measurements of  $U_{\pi 1,2}$  (T) and  $D_{\pi}$ (T) obtained below (Fig. 1) and above (Fig. 3) RT region indicates a rather wide temperature range of 150–400 K where relatively slight changes of  $U_{\pi 1,2}$  and  $D_{\pi}$  are observed. This range is larger than the actual operating temperature range of the most modern products of pyroelectric industry including domestic appliances, devices for scientific, security and paramilitary purposes. The changes of  $U_{\pi 1,2}$  (T) and  $D_{\pi}$ (T) are linked to the change of the pyroelectric figures of merit  $M_1 = \gamma/c_1$ ,  $M_2 = \gamma/c_1\epsilon$  and  $M_1/M_2 = \epsilon$ . The values of these changes, relatively to RT, are respectively equal to 21%, 9% and 12% in LiNbO<sub>3</sub> crystals and to 24%, 7% and 17% in LiTaO<sub>3</sub> crystals. The data supported deduced from direct measurements of pyroelectric charge release (Fig. 4) yield a maximum value of about 18% in the change of pyroelectric coefficient for LiNbO<sub>3</sub>.

The values of  $M_{1,2}$  at RT for LN are  $M_1 = 2,5 \cdot 10^{-11}$  A·m/W,  $M_2 = 0,8 \cdot 10^{-12}$  C·m/J and for LT are  $M_1 = 5,5 \cdot 10^{-11}$  A·m/W,  $M_2 = 1,3 \cdot 10^{-12}$  C·m/J. These values are in a good agreement with known data [3].

Slight changes of  $\gamma$  and  $M_{1,2}$  in the wide temperature range are connected to the variation of current  $R_A$  and voltage  $R_V$  responsivities of SE ( $R_A \propto M_1$  and  $R_V \propto M_2$  [3]), leading to a better satisfaction of requirements for PDR temperature stabilization systems.

As it is shown in reference [3] the noise equivalent power (NEP) can be written, in the pyroelectric voltage mode, as  $NEP_v = P_{N2} \propto (c_1/\gamma)(dA/\rho)^{1/2}$  and in the current mode  $NEP_I = P_{N1} \propto (c_1/\gamma)d/(R_1)^{1/2}$ .  $d$  is the thickness of SE,  $\rho$  is the resistivity,  $R_1$  is the load resistance. We can notice that the  $d$  value variation affects the NEP and  $D^*$  values more strongly in the pyroelectric current mode than in the pyroelectric voltage mode.

#### 4.2. Low-Temperature PDR

Concerning LN and LT application in low-temperature PDR it is reasonably first of all to concentrate our attention on the low-temperature maxima of  $U_{\pi 1,2}(T)$  (Fig. 1).

Diffuseness of the maxima in the temperature range 40–80 K could be considered as an advantage for choosing the temperature operation of PDR.

The increase of  $U_{\pi 1,2}(T)$  values in the range of low-temperature maximum corresponds to the increase of  $R_{A,V}$  and thus determines the corresponding increase of  $D^*$  and decrease of  $P_N$  values.

Figure 5 presents the temperature variations of  $D^*$  and  $P_N$  of SE based on LN and LT thin plates ( $d = 20 \mu\text{m}$ ,  $A = 1 \text{ mm}^2$ ) at  $f_m = 20 \text{ Hz}$  under  $1 \text{ M}\Omega$  and  $10 \text{ G}\Omega$  load resistor values.

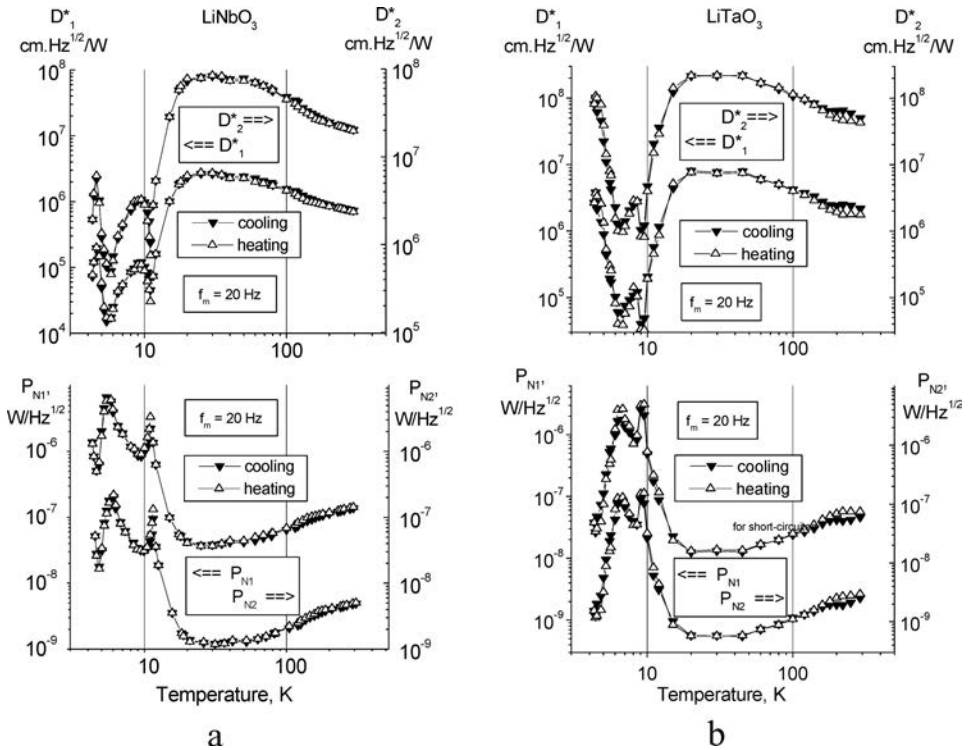


**Figure 5.** Dependences  $D^*_{1,2}(T)$  (upper part) and  $P_{N1,2}(T)$  (lower part) of SE of PDR based on  $\text{LiNbO}_3$  (a) and  $\text{LiTaO}_3$  (b) under cooling and heating runs in the temperature range of 4,2–290 K.

We can see that the temperature dependence follows the law described by the relationship  $U_n(T) \propto \sqrt{T}$  [3]. Due to the increase of the sensitivity and to the decrease of the temperature, the signal-to-noise ratio value increases 2-4 times in comparison with its value at RT. It is worth noticing that in a number of cases for getting sufficient thermal resolution three-times decrease of NEP is sufficient.

The enhancement of the detectivity  $D^*$  of PDR requires:

- FET operating at low source-gate and source-drain voltages for decreasing  $U_n$  of FET [16];
- Transistors operating at micro-power mode [17] for decreasing general power consuming, heat evolution and thermal drift of SE of PDR;
- FET operating at temperature down to 4,2 K [18].

Low-temperature PDR find their most effective application in the space vehicle destined for deep space probing. Indeed, in this case the ideal conditions of operation are fulfilled (nearly no natural sources of thermal and photoactive irradiation) leading to minimal energy consuming and high sensitivity of the detector.

### 4.3. Pyroelectric Sensors Based on $\gamma$ Sign Change Phenomenon

We have seen on Fig. 1 that for both LN and LT crystals, a  $180^\circ$ -change of  $\varphi_{\pi 1,2}(T)$  corresponding to a change of the sign of the pyroelectric coefficient  $\gamma$ .

In reference [8] we have demonstrated that the peculiarities of  $\gamma$  sign change phenomena (the absence of sign change of  $\gamma(T)/c_1(T)$ , sign change of  $\gamma(T)^*/c_1^*(T)$  and two sign changes of  $\gamma(T)^*/c_1^*(T)$ ) arise principally from the striction coefficients corresponding to the average of the whole possible lattice distortions and thus depend on defect subsystem. These defects can be the impurities and the non-stoichiometry of the crystals. An another kind of defect concerns the interaction of ferroelectric self-induced distortions, under the action of internal organizing factors (such as pyroelectric fields), with the crystal lattice itself.

The effect of  $\gamma(T)$  sign change can be used for the realization of zero-principle based pyroelectric amplitude-phase converters.

The deviation of the temperature of the SE from  $T_0$  under absorption of the energy of thermal flux or incident irradiation can be compensated by using direct heating or radiation heating (resistive heater or LED) and  $U_{\pi 1,2}(T)$  and  $\varphi_{\pi 1,2}(T)$  as an zero-indicator.

Some applications of the effect of the  $\gamma$  sign change can be proposed [5, 7, 20]:

- Temperature stabilization of pyroelectric SE operating in the vicinity of  $T_0$ .
- High accuracy measurement of the thermal flux intensity by observing a change in  $U_{\pi 1,2}$  and  $\varphi_{\pi 1,2}$ .
- Non-isothermal position-sensitive PDR by placing the pyroelectric SE in a temperature gradient parallel to the irradiated surface and by adjusting the temperature  $T_0$  of the middle part of this surface.

The effect of the change of the pyroelectric coefficient sign can be used for metrological purposes, such as the control of spatial position of IR-beams and in systems of IR-orientation.

## 5. Conclusion

The obtained results show that LN and LT single crystals are suitable for:

- i) PDR operation in the range 200–400 K with slight temperature changes of  $U_\pi$  and  $\gamma$  values and for which the difference in  $U_{\pi 1,2}(T)$  under cooling-heating runs is minimal in comparison with other pyroactive single crystals used in IR-sensing;
- ii) low-temperature PDR in the range 40–80 K with low-temperature  $U_\pi(T)$  maxima;
- iii) zero-principle based PDR and position sensitive PDR and also pyrosensors for temperature stabilization based on the effect of  $\gamma$  sign change in the range 4,5–12 K.

The improvement of such devices passes through the control of the crystal defect structure. Cryogenic treatment influences the behavior of  $U_{\pi 1,2}(T)$  in the vicinity of the low-temperature  $U_{\pi 1,2}(T)$  maxima (40–80 K) and in the vicinity of 200 K.

LN and LT crystals are among the best ones for creating various types of high sensitive reliable PDR in a wide temperature range including low temperatures.

## Acknowledgments

The work was supported by Université de Valenciennes et du Hainaut-Cambrésis and by Université de Metz et Supélec.

## References

1. Yu. S. Kuz'minov, Niobate and tantalate of lithium materials for nonlinear optics (in Russian). Moscow: Nauka (1975).
2. M. E. Lines and A. M. Glass, Principles and Applications of Ferroelectrics and Related Materials. Oxford: Clarendon Press (1977).
3. L. S. Kremenchugsky and O. V. Roitsina, Pyroelectric Detectors of Radiation (in Russian). Kiev: Naukova Dumka (1979).
4. A. M. Glass and M. E. Lines, Low-temperature behavior of spontaneous polarization in  $\text{LiNbO}_3$  and  $\text{LiTaO}_3$ , *Phys Rev B* **12**, 180–191 (1976).
5. S. L. Bravina, L. S. Kremenchugsky, N. V. Morozovsky, and A. A. Strokach, Experimental and theoretical investigation of the pyroelectric effect in ferroelectric crystals at low temperatures. *Ferroelectrics*. **118**, 41–50 (1991).
6. S. L. Bravina and N. V. Morozovsky, Pyroelectricity in some ferroelectric semiconductors and its applications. *Ferroelectrics*. **118**, 217–224 (1991).
7. S. L. Bravina, N. V. Morozovsky, and A. A. Strokach, Pyroelectricity: some new research and application aspects. In: Sizov FF, ed. Material Science and Material Properties for Infrared Optoelectronics. Bellingham: SPIE; **3182** 85–99 (1997).
8. S. L. Bravina, A. N. Morozovska, N. V. Morozovsky, YuA Skryshevsky, Low-temperature pyroelectric phenomena in lithium niobate single crystals. *Ferroelectrics*. **298**, 31–42 (2004).
9. R. L. Byer and C. B. Roundy, Pyroelectric coefficient direct measurement technique and application to a nsec response time detector. *Ferroelectrics*. **3**, 333–338 (1972).
10. S. A. Gridnev, V. I. Popov, A. S. Loginova, Investigation of stability of piezoelectric materials at helium temperatures. In: Ferroelectrics and Piezoelectric. Kalinin: KGU 16–22 (1984).
11. S. L. Bravina, N. V. Morozovsky, and Yu. A. Skryshevsky, Pyroeffect and thermostimulated phenomena in crystals of TGS family. *Sol. St. Phys.* **32** 2543–2548 (1990).
12. S. L. Bravina, N. V. Morozovsky, A. K. Kadashchuk, and N. I. Ostapenko, Pyroelectric phenomena in lithium metagermanate. *J. Techn. Phys.* **60**, 97–101 (1990).
13. S. L. Bravina, N. V. Morozovsky, A. K. Kadashchuk, and V. S. Manzhara, Low temperature pyroelectric and luminescence phenomena in  $\text{Sn}_2\text{P}_2\text{S}_6$  single crystals. *Ferroelectrics*. **192**, 197–201 (1997).
14. B. K. A. Mirza, P. D. Townsend, and G. L. Destefanis, Light emission from the surface of  $\text{LiNbO}_3$ . *Phys Status Solidi*. **A47**, K63–K66 (1978).

15. G. I. Rosenman, I. S. Rez, Yu L Tshepelev, N. B. Angert, and E. I. Boikova, Exoemission and electret effect in lithium niobate crystals. *J Techn Phys.* **52**, 1890–1892 (1982).
16. N. V. Morozovsky, V. B. Samoilov, and I. A. Stoyanov, Investigation of matching stages for pyroelectric detectors of radiation. In: Thermal Detectors of Radiation. *Leningrad: GOI*; 104–105 (1980).
17. D. V. Igumnov, Basis of micro-power electronics (in Russian). Moscow; MIREA; (1974).
18. B. Lengeler, Semiconductor device suitable for use in cryogenic environments. *Cryogenics.* **8**, 439–447 (1974).
19. V. N. Novikov, V. K. Novik, A. B. Esengaliev, and N. D. Gavrilova, Point defects and singularities of the low-temperature ( $T < 15\text{K}$ ) behavior of pyroelectric coefficient and the spontaneous polarization of the TGS,  $\text{LiTaO}_3$  and  $\text{LiNbO}_3$ . *Ferroelectrics.* **118**, 59–69 (1991).
20. S. L. Bravina, N. V. Morozovsky, and A. A. Stokach, Effect of the sign of pyroelectric coefficient change and: possibility of its application for registration of thermal radiation. In: Thermal Detectors of Radiation. *Leningrad: GOI*, 82–83 (1990).